High K Dielectric Resonator Antenna

NICOLAESCU IOAN[1], IOACHIM ANDREI [2], TOACSAN IRINA[2], RADU IONUT[1], BANCIU GABRIEL[2], NEDELCU LIVIU[2]
Military Technical Academy [1],
National Institute for Materials Physics[2] , Bucharest
81-83, George Cosbuc Avenue, Bucharest[1]
105 bis Atomistilor Street, Bucharest-Magurele[2]
ROMANIA
ioannic@mta.ro http://www.mta.ro

Abstract: - The microwaves are used for both civilian and military applications for communications and detection. In the communication area, the endeavours of the scientist are focused to increase both the quantity and the quality of the data send over a communication link. The need to increase the amount of data that can be handled by a communication system is requested by the desire to use a communication device not only for voice but also for data, images, pictures and video transmission. Sending video over a communication link needs more bandwidth, which may be provided by increasing the operational frequency. In this way the frequency range of communications systems have extend from hundreds of KHz to MHz and now to microwaves (ISM band, IEEE 802.11 standard, Wi-MAX etc). The quality of the data is assured by improving the processing methods such as modulation, different methods of coding for digital systems, spatial processing (MIMO systems etc) etc. In addition to increased demand for bandwidth and quality there is a strong requirement for multifunction and miniaturised communication devices, which can be provided by using special designed microwave materials. In the field of detection devices the applications range from radar systems to microwave imaging systems, anti-collision systems, ground penetrating radar etc. In this case, the miniaturisation is a very important issue, too. As it is know the size of different kind of microwave components is in a certain relation with the wavelength divided by root square of the dielectric permittivity. Therefore, the size of the microwave component can be decreased by increasing the dielectric permittivity. Dielectric materials based on TiO_2 are suited for applications in electromagnetism and optics due to their nonlinear properties, their high value of the dielectric permittivity and their temperature behaviour.
The paper describes very shortly the technology applied to manufacture high dielectric permittivity materials based on TiO_2 and a dielectric resonator antenna manufactured with these materials. The experimental data measured for dielectric antenna are presented.

Key-Words: - high K dielectric materials, dielectric resonators, antennas

1. Introduction

Last technological developments in the field of wireless communication and radar systems led to one of the most spectacular development of dielectric materials technologies and microwave devices. Thus, dielectric materials are used to manufacture passive microwave devices such as filters, resonators and antennas. Also new types of technologies and materials are used to improve the integration of microwave systems. Among these, a great interest for high K dielectric materials is in connection with the main requirements for microwave passive devices:
1. The miniaturization is one of the most important demand and it supposes to manufacture dielectric compositions with very high dielectric permittivity (ε_r)in order to decrease both the size and the weight of microwave devices.
2. The thermal stability of the parameters is another very important issue. Usually the temperature varies from -40^o to +100^{o}C and in this range the resonance frequency has to change no more than 10ppm/^{o}C. This thermal variation depends on the temperature coefficient τ_ε by:

$$\tau_f = -1/2\,\tau_\varepsilon - \alpha\,; \qquad (1)$$

where α is the thermal expansion coefficient. As one can notice in the above formula τ_f is dominated by τ_ε that changes from –2000 to +2000 ppm/^{o}C on dielectric materials with ε_r > 30. As a result there are very few materials, which can be used in these applications.

3. The dielectric losses ($\tan\delta$) should be very low, so the quality factor has to be higher than 1000.
Due to the intrinsic properties discussed above, the dielectric resonators (DR) are very attractive for oscillator and filter design. However, in recent years the use of high dielectric materials as DRs antennas is of great interest [1].
Various geometries of dielectric resonator antennas offer significant volume reduction making them potential candidates for use in compact applications such as mobile communication handsets. There are, also, applications where several DR antennas are combined into an array to improve the performances of the system. In this case the size of the array is very important and using high K dielectric materials contributes to decreasing both the dimension of the system and the coupling signal between two adjacent antennas.

2. Dielectric material (barium neodymium titanate -BNT) description

The BNT dielectric materials, which are compositions based on BaO - Nd_2O_3 – TiO_2 ternary system, are very attractive for microwave devices due to their high dielectric constant and low losses in the microwave frequency range [1-3]. These materials exhibit a dielectric constant in the range of $\varepsilon_r = 70 \div 80$, depending on the Nd_2O_3 and TiO_2 content. In principle, the addition of highly polarisable ions can increase dielectric permittivity of BNT materials. For this reason, the Pb effect, which substitutes the Ba ions, on the dielectric parameters was investigated for $Ba_{1-x}Pb_xNd_2Ti_5O_{14}$ compounds. When Pb is added to the BNT, the dielectric constant is increased to $80 \div 90$ with a slight increase in dielectric loss. The lead addition changes also the temperature coefficient τ_f [4]. The temperature coefficient of the resonance frequency f_o of a dielectric resonator is defined by

$$\tau_f = \frac{1}{f_0}\frac{\Delta f}{\Delta t}, \qquad (2)$$

where Δf is the shift in the resonance frequency for a Δt temperature variation.
Samples of different Nd_2O_3 concentrations in the range of 0÷30 wt % were investigated in order to study the modifications of the BNT ceramics structural and dielectric properties with the increase of the Nd content [5].
Structural characteristics of some BNT ceramics are shown in Table 1. A typical X-ray diffraction (XRD) pattern shown in Fig. 1 contains the diffraction lines of $BaNd_2Ti_5O_{14}$ with the specific orthorhombic structure as dominant phase and few peaks that can be attributed to $BaTi_4O_9$.
The crystallite mean dimension (*D*) was calculated from the formula $D(\mathring{A}) = k\lambda(\mathring{A})/\beta\cos\theta$, where β is half of the line width (rads), θ is the Bragg angle, and *k* a constant depending on the crystallites shape. In a spherical coordinate system, $k = 1.0747$ for crystalline plans with Miller indices (*hkl*) greater than 110.
It can be noticed:
1 - A decrease of the interplanar distances, which corresponds to an increase of 2θ angles, due to the increase of the Nd concentration,
2 – The density measured by pycnometric method (in water) decreases with the increases of Nd concentration,
3 - The crystallites mean dimension (*D*) shown in the last column of Table 1, increases with the increase of Nd concentration. However, these dimensions do not reach the crystallite dimension of pure material ($BaTiO_3$) due to some other additives.

Table 1. Structural and densification data of BNT compounds (without Pb addition) sintered at T_s = 1250°C/2.5 h as function of Nd content; ρ is the ceramic density, θ is the Bragg angle, and *D* the crystallite mean dimension.

Sample	Nd_2O_3 (wt %)	ρ (kg/m^3)	2θ	D (μm)
BNT 0 ($BaTiO_3$)	0	5490	31.71	4.10
BNT 2	2	5070	31.73	2.65
BNT 4	4	4930	31.77	3.04
BNT 6	6	3690	31.82	3.57
BNT 10	10	3570	31.759	3.72
BNT 20	20	3590	31.759	3.89

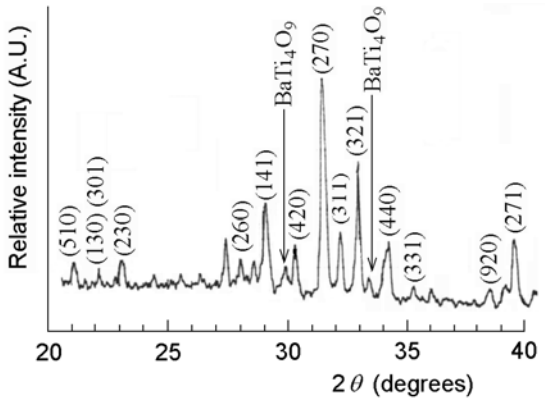

Fig. 1. X-ray diffraction pattern for BNT ceramic with 0.28 wt % Nd_2O_3 and 0.5 mol Pb ceramic sintered at 1250/2h

The Pb addition is a way to obtain a desired value of τ_f. A controllable τ_f is another feature that makes $Ba_{1-x}Pb_xNd_2Ti_5O_{14}$ materials very attractive to microwave applications.

3. Preparation of dielectric material

The $Ba_{1-x}Pb_xNd_2Ti_5O_{14}$ samples [6] based on BaO-PbO-Nd_2O_3-TiO_2 system were prepared by the solid-state reaction technique. The starting materials TiO_2, PbO, Nd_2O_3, and $BaCO_3$ powders of purity higher than 99 % were weighted for the desired stoichiometry. The raw materials were ball-milled in water for two hours and then calcined at 1200 ^oC. The powder was crushed and milled again for 2 hours. Mixing was carried out for 2 hours in an agate mortar with agate balls. The mixture was pressed into pellets, which were sintered at temperatures between 1230^0C and 1260^0C for 2 hours. In order to obtain high densities at low sintering temperatures, 0.2 wt % NiO was added for some samples. The NiO sintering addition acts as a grain-growth inhibitor improving the quality factor Q_o in microwave domain. The bulk densities of the sintered pellets were measured by Archimede's method. Structural and morphological analyses were performed on $Ba_{1-x}Pb_xNd_2Ti_5O_{14}$ samples by X-ray diffraction (XRD) analysis, and electron microscopy (SEM). The patterns were recorded in a 2θ range from 20^o to 60^o on a Seifert Debye Flex 2002 diffractometer into the $2\theta - \theta$ mode. Measurements were performed at room temperature using a Ni - filtered Cu K_α radiation, and a counter scan speed of 5^o/min. $Ba_{1-x}Pb_xNd_2Ti_5O_{14}$ samples with $x = 0$, 0.33 and 0.5 Pb content were investigated in order to study the modifications on morpho-*structural* and dielectric properties of the BNT: Pb ceramics with the increase of the Pb concentration. The sintered ceramics were polished and etched in order to remove the surface layer and to obtain plan parallel surfaces. A good compactness was obtained for rectified samples for all sintering temperatures.

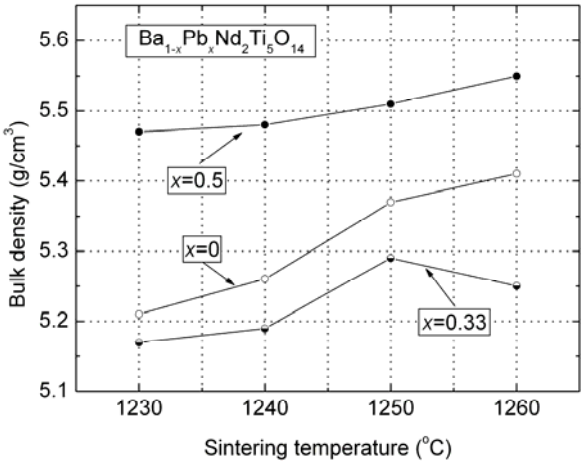

Fig 2. Bulk density versus sintering temperature of $Ba_{1-x}Pb_xNd_2Ti_5O_{14}$ samples.

The bulk density versus sintering temperature of $Ba_{1-x}Pb_xNd_2Ti_5O_{14}$ samples is shown in fig. 2.
Structural investigations of $Ba_{1-x}Pb_xNd_2Ti_5O_{14}$ ceramics were made using XRD. For $x = 0$, the X-ray diffraction pattern shown in fig. 3 contains the diffraction lines of the single-phased $BaNd_2Ti_5O_{14}$ with the orthorhombic structure. With the increase of the Pb content x, the XRD peaks intensity increases and the secondary-phase $Nd_4Ti_9O_{24}$ appears.

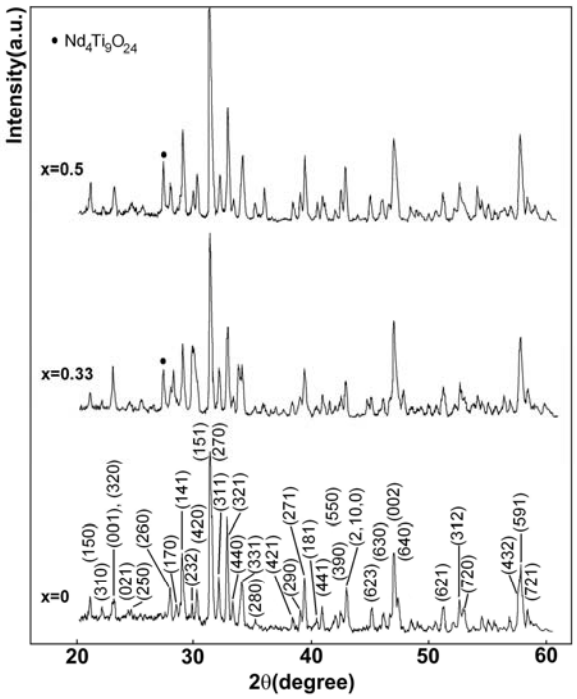

Fig. 3, X-ray diffraction patterns for $Ba_{1-x}Pb_xNd_2Ti_5O_{14}$ ceramic samples sintered at 1250/2h.

The SEM morphology of $Ba_{1-x}Pb_xNd_2Ti_5O_{14}$ samples sintered at 1250 °C for 2 hours is shown in figs. 4-6.

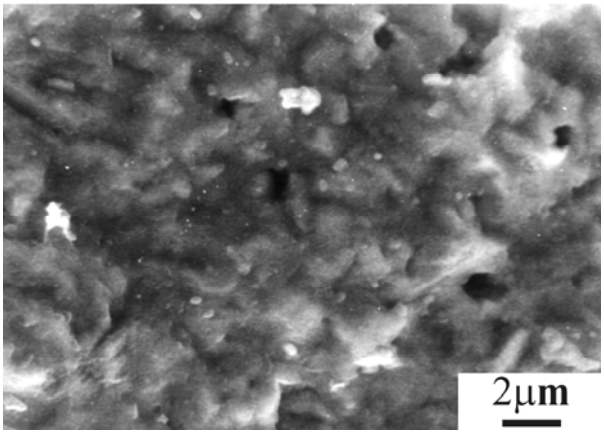

Fig. 4. SEM image of $BaNd_2Ti_5O_{14}$ sintered at 1250 °C for 2 hours.

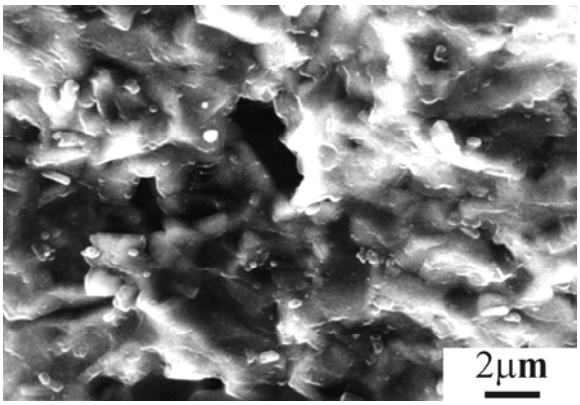

Fig. 5. SEM image of $Ba_{0.66}Pb_{0.33}Nd_2Ti_5O_{14}$ sintered at 1250 °C for 2 hours.

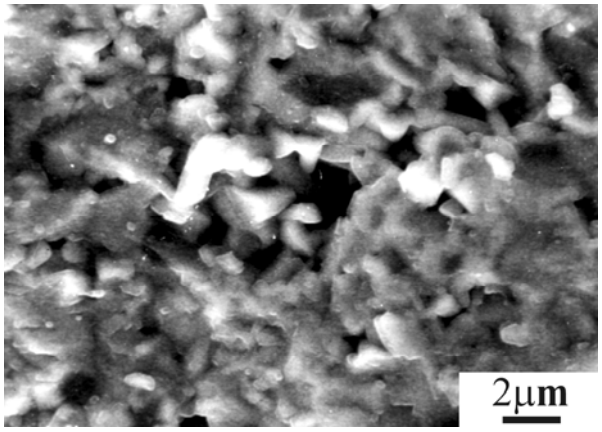

Fig. 6. SEM image of $Ba_{0.5}Pb_{0.5}Nd_2Ti_5O_{14}$ sintered at 1250 °C for 2 hours.

Spherical or polyhedral grains and pores appear in all the images. The size of the grains (1÷8 μm) increases with the increase in the Pb concentration. For samples with $x = 0$ or 0.33 Pb content, the crystallites dimensions vary between 0.5 and 3 μm (Fig. 4 and Fig. 5). At $x = 0.5$ Pb concentration, the large aggregates with dimensions $d > 10$ μm bonded by high sizes pores disappear, as can be seen in Fig. 6. For samples with $x = 0.5$, the ceramics exhibit a good densification due to the high crystallites size in the range 2 ÷ 4 μm.

4. Dielectric properties

In order to investigate the neodymium content effect on the ferroelectric - paraelectric transition, $Ba_{1-y}Nd_yTiO_3$ samples were sintered at 1350 °C for 2 hours with $y = 0.01$, 0.03 and 0.05 Nd content. The ferroelectric transition temperature and the dielectric constant decrease with the increasing Nd content. These results are presented in fig. 7.

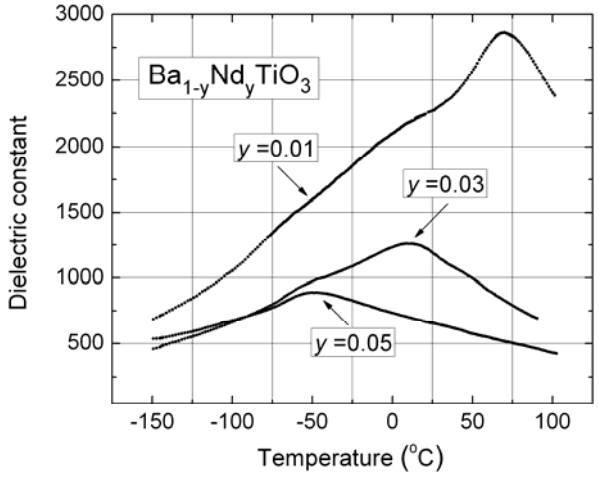

Fig. 7. Temperature dependence of dielectric constant measured at 1 kHz for $Ba_{1-y}Nd_yTiO_3$ samples sintered at 1350 °C for different Nd contents.

The Nd effect on $Ba_{1-y}Nd_yTiO_3$ properties is to depress the ferroelectric–paraelectric transition to lower temperatures, depending on the Nd concentration. At $y = 0.01$, the transition temperature T_c is around 70°C. A transition temperature at $T_c \sim 10$°C was observed for the sample with $y = 0.03$. The BNT sample with $y = 0.05$ exhibits a slow decrease of the dielectric constant with the temperature increase, which indicates a region far from the ferroelectric-paraelectric transition ($T_c \sim -50$ °C). The microwave measurements were performed in the 2÷5 GHz frequency range by using Hakki-Coleman method [7]. A plot of few resonating modes of a $Ba_{0.5}Pb_{0.5}Nd_2Ti_5O_{14}$ dielectric resonator of 18.15 mm diameter and 10.78 mm height, placed in a Courtney holder, is depicted in fig.. 8. In order to accurately correct for the coupling losses, the external couplings were reduced and the TE_{011} resonance peak was investigated not very far from the noise floor. Corrections for the conduction losses in the parallel plates were considered also for accurate measurements of the dielectric resonator intrinsic quality factor Q_o.

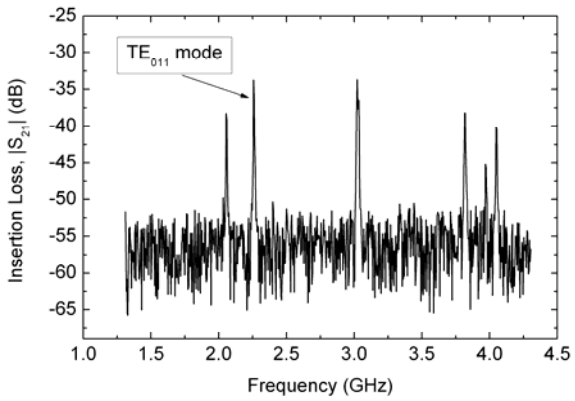

Fig. 8. Resonance peaks in microwave range of a $Ba_{0.5}Pb_{0.5}Nd_2Ti_5O_{14}$ dielectric resonator with 18.15 mm diameter and 10.78 mm height.

The microwave measurements on $BaNd_2Ti_5O_{14}$ samples, which do not contain Pb, show an increase of the dielectric constant with the increase in the sintering temperature as shown in table 2. However, the quality factor exhibits a maximum value for the samples sintered at 1250°C for 2 hours.
For an $x = 0.33$ Pb content, the dielectric constant increases with the increase of the sintering temperature as shown in table 3. Nonetheless, the variation of the $Q \times f_o$ is in correlation with the variation of the bulk density showed in fig.. 2.
The temperature coefficient τ_f takes slightly smaller values as in the case of $BaNd_2Ti_5O_{14}$. The highest values of the dielectric constant were achieved for $Ba_{0.5}Pb_{0.5}Nd_2Ti_5O_{14}$ samples (table 4).
The dielectric constant somewhat increases with the sintering temperature.
The dielectric constant in microwave range can be correlated with the bulk density: both parameters exhibit the highest values for $x = 0.5$ and they both increases with the increase in sintering temperature.

Table 2. Microwave characteristics of the $BaNd_2Ti_5O_{14}$ samples versus sintering temperature.

Sample	T_s/ t_P (°C/h)	ε_r	Q_o f_o (GHz)	τ_f ppm/°C
1	1230/2	76.1	7978	+60 ÷ +70
2	1240/2	76.8	8148	
3	1250/2	78.2	8890	
4	1260/2	79.3	7350	

Table 3. Microwave characteristics of $Ba_{0.66}Pb_{0.33}Nd_2Ti_5O_{14}$ versus sintering temperature

Sample	T_s/ t_P (^oC/h)	ε_r	Q_o f_o (GHz)	τ_f (ppm/^oC)
5	1230/2	81.6	6780	+50 ÷ +55
6	1240/2	83.5	6625	
7	1250/2	83.4	5734	
8	1260/2	85.3	6364	

Table 4. Microwave characteristics of $Ba_{0.5}Pb_{0.5}Nd_2Ti_5O_{14}$ versus sintering temperature.

Sample	T_s/ t_P (^oC/h)	ε_r	Q_o f_o (GHz)	τ_f (ppm/^oC)
9	1230/2	84.2	5040	-10 ÷ -15
10	1240/2	85.1	5270	
11	1250/2	86.5	5240	
12	1260/2	86.6	5170	

Furthermore, the lowest value of the temperature coefficient $|\tau_f| < 15$ ppm/^{o}C was achieved for the $Ba_{0.5}Pb_{0.5}Nd_2Ti_5O_{14}$ samples. However, the quality factor, which practically does not depend on the sintering temperature, is smaller as in the previous cases for $x = 0$ or $x = 0.33$.

The main applications of these materials are:

- dielectric resonators (DR);
- planar and dielectric resonator antennas.

5. Dielectric resonator antenna

The dielectric antenna is used for application where there is no much space available and there are special mechanical requirements. So, it will be found on missiles, aircrafts, UAV etc. The antenna can be found as a dielectric stick, when the dielectric permittivity is relatively low (it behaves as a dielectric waveguide, which radiates the electromagnetic energy) and as a dielectric resonator, when the dielectric permittivity is high. The intrinsic quality factor of a dielectric resonator may be as high as 20.000 for frequencies from 2 to 20 GHz and the product Qf between the quality factor Q and the frequency f does not depend upon the frequency for a wide frequency range. The operation principle of the dielectric resonator can be understood by studying the electromagnetic waves propagation through a circular dielectric waveguide. Transversal electric TE_{0n}, transversal magnetic TM_{mn} and hybrid electromagnetic HEM_{mn} modes can exist in a dielectric waveguide. The first index m shows the number of complete cycles of the field in the plane of the cross-section horizontal plane and the second index n indicates the number of radial cycles. For the transversal electric and transversal magnetic modes, the first index m is 0 and the field is circularly symmetrical. As an example, the field distribution in the cross-section of the dielectric circular waveguide is shown for the TE_{01} mode, TM_{01} and HEM_{01} in figures 3, 4 and 5, respectively. The hybrid HEM_{mn} modes exhibit both electric and magnetic axial components. As known, such hybrid modes cannot exist in conventional metallic waveguides and this aspect is a major difference between the dielectric waveguides and the closed metallic waveguides.

When a section of the dielectric waveguide is used as a resonant cavity a standing wave regime is obtained. This device is called dielectric resonator and TE_{0np}, TM_{0np} and HEM_{mnp} resonance modes can exist. The third index p is an integer greater or equal to unity and is used to show the number of half wavelengths in the axial direction of the waveguide.

In practice, one of the most used modes is $TE_{01\delta}$. Here the third index, δ, is a positive real number, less than unity, and denotes that the length of the dielectric resonators is less then a quarter of a wavelength. The actual values depend on the value of the dielectric constant of the material, on the substrate and on the separation between the two conductive planes. Usually the value of δ is not specified because it is not necessary.

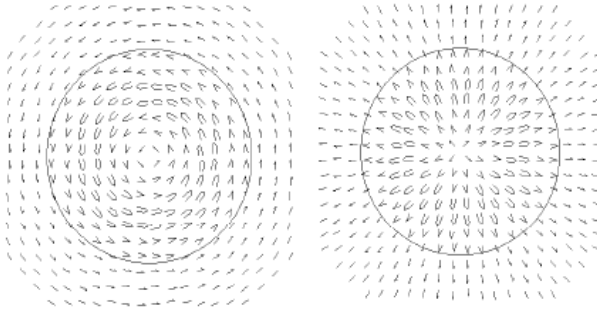

Fig. 9. TE_{01} in dielectric waveguide, left E field and right H field.

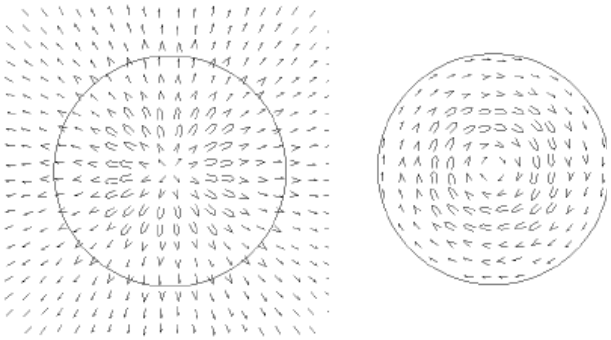

Fig. 10. TM_{01} in dielectric waveguide, left E field and right H field.

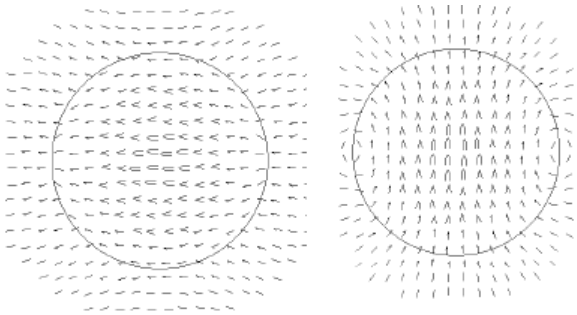

Fig. 11. HEM_{01} in dielectric waveguide, left E field and right H field.

When a dielectric resonator is not fully protected by a metallic surface, it may radiate and became an antenna. As can be seen on figure 12 the dielectric resonator is fixed on the metallic surface and the inner conductor of the feeding coaxial cable excites the antenna.

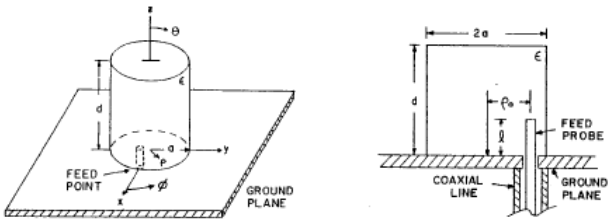

Fig. 12. Dielectric antenna fed with coaxial probe [5]

In [6] it had been demonstrated that the resonance frequencies are complex:

$$s_{m,n} = \sigma_{m,n} + j\omega_{m,n} \quad , \tag{6}$$

and that each solution corresponds to a resonant mode *m,n* which satisfies the continuity condition on the frontier. The ratio between real part and imaginary part is the quality factor:

$$Q_r = -\frac{\omega_{m,n}}{2\sigma_{m,n}} \tag{7}$$

The minus sign shows that all passive circuits have their natural frequency on the left side of the complex plan, such as $\Gamma_{m,n}$ is a negative number, too. The natural frequencies as well as *Q* factors are presented in table no. 2.

Table 5. Resonance frequencies and Q factors for a dielectric resonator antenna ε_r=38, *a*=5,25mm and *h*=4,6mm [6]

Mode	f_r[GHz]	Q_r
TE_{01}	4.829	45.8
HEM_{11}	6.333	30.7
HEM_{12}	6.638	52.1
TM_{01}	7.524	76.8
HEM_{21}	7.752	327.1

The resonance frequency and the quality factor can be determined knowing the dimensions of the resonator and the value of the dielectric permittivity [9]. For instance the resonance frequency for HEM_{11} mode for a resonator having the radius a and the length h may be computed from formula:

$$k_0 a = \left(1{,}6 + 0{,}513x + 1{,}392x^2 - 0{,}575x^3 + 0{,}088x^4\right) / \varepsilon_r^{0{,}42} \tag{4}$$

where k_0 is free space propagation constant and $x=a/h$. Likewise he value of Q_r will be given by:

$$Q_r = x \cdot \varepsilon_r^{1,2}\left(0{,}01893 + 2{,}925e^{-2{,}08(1-0{,}08x)}\right). \tag{5}$$

6. Experimental results

Based on the technology described above a dielectric material with dielectric permittivity of 86 had been design and manufactured. It was used to make dielectric resonators of different dimensions (10X16 and 10X18 mm). The resonance frequency for 10X18 mm resonator was measured using a vector network analyzer and the S parameters can be seen on figure 13 where one can notice that the resonance frequency of a resonator is around 1000 MHz.

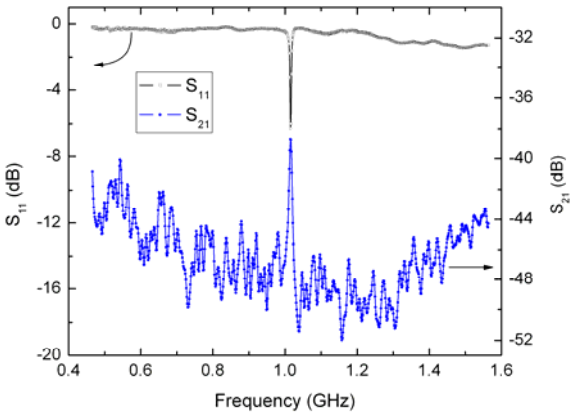

Fig. 13. S_{11} and S_{21} for dielectric resonator antenna.

A sketch of the resonator antenna is presented on figure 14. It is made from one or more resonator that are placed above a metallic plate in order to obtain a unidirectional antenna pattern. The dimensions of the metallic plate are 75X75 mm and it is large enough in comparison with the wavelength, which is around 30 cm). The antenna is fed using a probe which is placed in the centre of the resonator or off the centre at a certain distance. A good match was got by a distance of 7.81 mm.

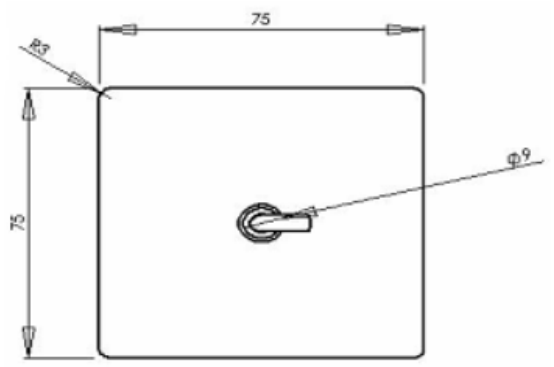

(a)

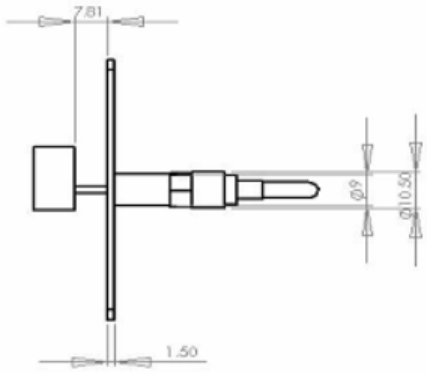

(b)

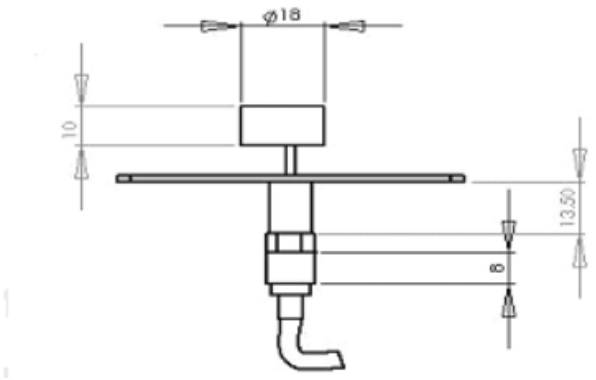

(c)

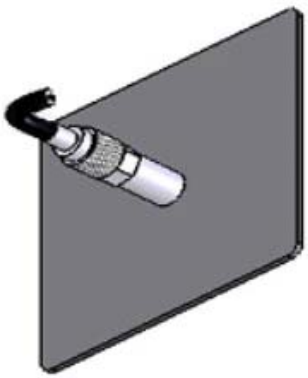

(d)

Fig. 14. Dielectric resonator antenna:
a) rear view; b) and c) side view; d) general view

Fig. 15. Dielectric resonator with the feeding point 3 mm off the center.

The measured pattern of the dielectric antenna with 3mm off the centre feeding point is presented on figure 16.

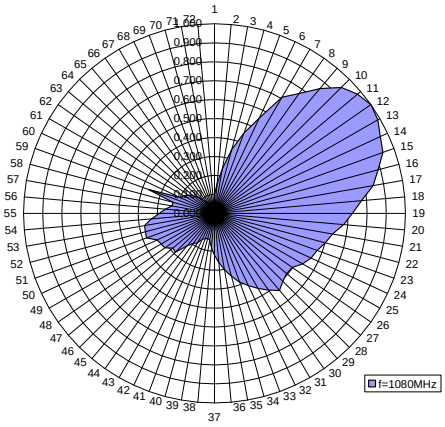

Fig. 16. Dielectric resonator antenna pattern

The voltage standing wave ratio of the antenna has been measured on the frequency range from 750 MHz to 1200MHz (fig.17).

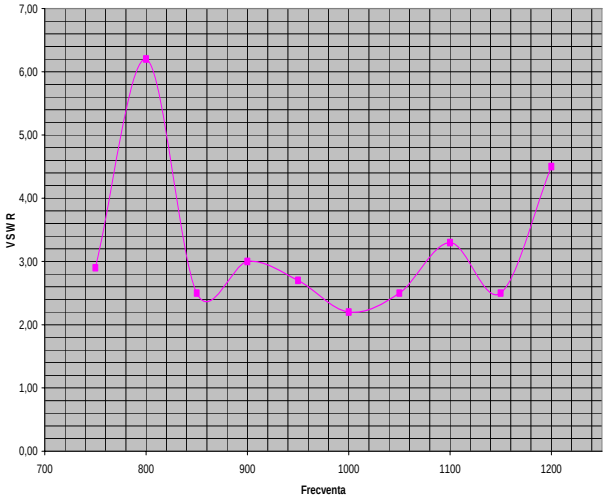

Fig. 17. Voltage standing wave ratio for a dielectric resonator antenna, from 750 MHz to 1200 MHz.

Another way to feed a dielectric antenna is on the centre of the resonator, as in figure 18.

Fig. 18. Dielectric resonator with central feeding point.

The measured pattern of the antenna in this case is displayed on figure 19.

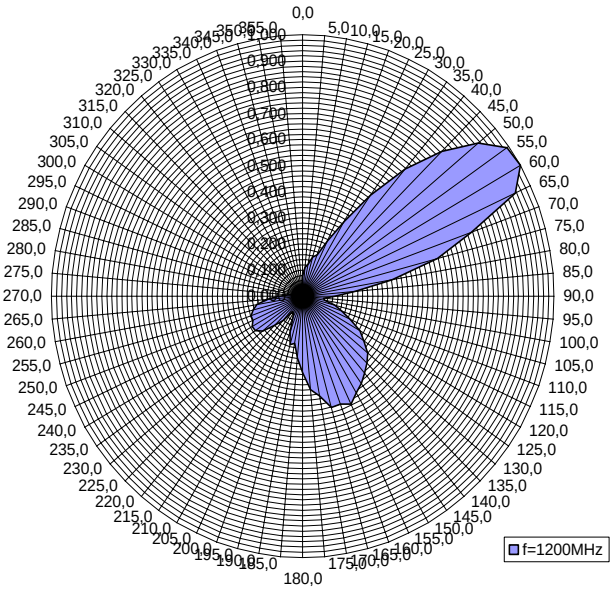

Fig. 19. Dielectric resonator antenna, central feed, for 1200 MHz.

Except one resonator antenna, measurements have been made using several resonators.